ACS NANO
Cite This: ACS Nano 2018, 12, 1050−1061
www.acsnano.org

ARTICLE

Influence of Salt on Supramolecular Oscillatory Structural Forces and Stratification in Micellar Freestanding Films

Subinuer Yilixiati, Rabees Rafiq, Yiran Zhang, and Vivek Sharma*

Chemical Engineering, University of Illinois at Chicago, Chicago, Illinois 60607, United States

Supporting Information

ABSTRACT: Freestanding films of soft matter containing micelles, nanoparticles, polyelectrolyte−surfactant complexes, bilayers, and smectic liquid crystals exhibit stratification. Stepwise thinning and coexisting thick−thin regions associated with drainage *via* stratification are attributed to the confinement-induced structuring and layering of supramolecular structures, which contribute supramolecular oscillatory structural forces. In freestanding micellar films, formed by a solution of an ionic surfactant above its critical micelle concentration, both interfacial adsorption and the micelle size and shape are determined by the concentration of surfactant and of added electrolytes. Although the influence of surfactant concentration on stratification has been investigated before, the influence of added salt, at concentrations typically found in water used on a daily basis, has not been investigated yet. In this contribution, we elucidate how the addition of salt affects stepwise thinning: step size, number of steps, as well as the shape and size of nanoscopic nonflat structures such as mesas in micellar foam films formed with aqueous solutions of anionic surfactant (sodium dodecyl sulfate (SDS)). The nanoscopic thickness variations and transitions are visualized and analyzed using IDIOM (Interferometry Digital Imaging Optical Microscopy) protocols with exquisite spatiotemporal resolution (thickness ∼1 nm, time <1 ms). In contrast to nanoparticle dispersions that show no influence of salt on step size, we find that the addition of salt to micellar freestanding films results in a decrease in step size as well as the number of stepwise transitions, in addition to changes in nucleation and growth of mesas, all driven by the corresponding change in supramolecular oscillatory structural forces.

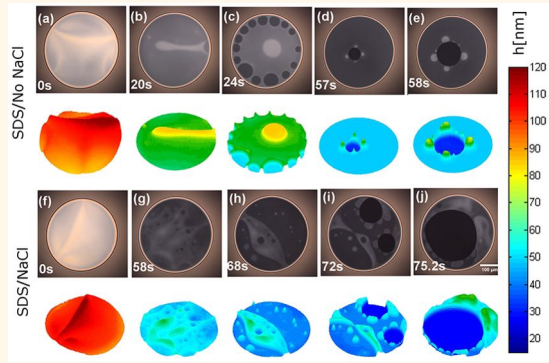

KEYWORDS: *micelles, foams, thin films, disjoining pressure, imaging, DLVO theory, surface forces*

Intermolecular and surface forces contribute a thickness-dependent disjoining pressure, $\Pi(h)$, that influences the stability of colloidal dispersions.[1−3] Early work by Derjaguin,[3,4] Scheludko,[5] Vrij,[6] and Mysels,[7] among others,[1−9] established that the surface forces also determine the stability of ultrathin freestanding[2,8,10,11] or supported[12−15] (at least one solid−liquid interface) films. Contributions due to dispersion forces (van der Waals, attractive), $\Pi_{vw}(h)$, and electrostatic double layer forces (repulsive), $\Pi_{el}(h)$, are often referred together as the Derjaguin−Landau−Verwey−Overbeek, or DLVO, forces.[2−8,10] Typically DLVO forces are said to delay or prevent the aggregation of proteins, macromolecules, particles, drops, bubbles, or lipid layers. In micelle-free foam films of ionic surfactants (concentration, c < CMC, or critical micelle concentration), drainage is marked by a monotonic decrease in thickness, culminating in the appearance of the "common black" (CB) films, as the thickness-dependent DLVO forces eventually counterbalance the capillary suction pressure.[3−7,10] Additional non-DLVO, shorter ranged, solvation forces are operative at nearly close contact[1] in colloidal dispersions, and in micelle-free foam films, these can lead to the appearance of a second black film called the "Newton black" film ($h \approx$ few nm). In contrast, drainage in micellar foam films proceeds *via* stratification that involves nonmonotonic, stepwise thinning[10,16−20] attributed to the role played by non-DLVO, supramolecular oscillatory structural forces.[10,19−22] The supramolecular oscillatory structural forces can be longer ranged than DLVO forces and can stabilize successive layers with a quantized difference in thickness of flat regions. In this article, we elucidate how the addition of salt affects stratification as well as the supramolecular oscillatory structural forces in micellar foam films formed by aqueous solutions of sodium dodecyl sulfate (SDS). The goals of the study are threefold: (a) analyze the variation of step size and the number of steps, (b) visualize and characterize the shape and size of nanoscopic nonflat

Received: July 29, 2017
Accepted: January 9, 2018
Published: January 9, 2018

DOI: 10.1021/acsnano.7b05391
ACS Nano 2018, 12, 1050−1061

structures like nanoridges and mesas, and (c) develop a phenomenological expression for supramolecular oscillatory structure forces, to further elucidate the thermodynamics of stratifying thin films.

Nikolov *et al.*[18] postulated that stratification in freestanding films containing micelles and latex particles has a similar origin. Furthermore, Nikolov *et al.*[18] observed that stratification in films containing charged micelles could be suppressed by adding a relatively high concentration of salt; for example, no stratification was observed above 90 mM NaCl for 30 mM SDS and 100 mM NaCl for 60 mM SDS. This single dataset (which is presented in multiple papers[16,18,23,24]) utilized salt concentrations that exceeded surfactant concentration; however, detailed datasets on change in step size or number of steps were not presented. In contrast, measurements for charged nanoparticles using stepwise thinning in freestanding films,[16−18,25] X-ray scattering,[26] electron cryomicroscopy,[27] and colloidal probe atomic force microscopy (CP-AFM)[26,28−31] as well as simulations[26,30] have established that the interparticle distance in bulk fluid, the step size in thin film drainage, and the measured period of oscillation in force−distance curves, are all equal to each other. Furthermore, for the charged nanoparticle dispersions, the step size depends only on the particle number density and is not affected by the addition of salt, even though the electrostatic interactions are dependent on the electrolyte concentration. Surprisingly, hardly any studies investigate or describe the influence of added salt on thickness transitions and variations in stratifying micellar films for lower salt concentrations, even though water samples from natural resources say river or lake water have salt concentration c_s < 50 mM, and salty human sweat contains c_s < 80 mM. Practically, an understanding of the influence of salt added at intermediate salt concentrations of 1 mM < c_s < 60 mM is crucial for controlling and characterizing the stability, lifetime, rheology, and properties of aqueous foams, as these are determined by stability and drainage in freestanding liquid films (and their junctions, called Plateau borders)[32−36] that keep gas pockets apart in a foam. The rheological response of foams, including viscous dissipation, depends upon film thickness, and elasticity depends directly on overall foam microstructure.[36−38] Quantifying and controlling the variations in film thickness over time are critical for designing foams with suitable shelf-life and flow behavior, and in this study, we make crucial progress toward elucidating the influence of salt or surfactant concentration on supramolecular oscillatory structural forces.

In reflected light microscopy, stratified micellar foam films show coexisting regions with different shades of gray due to thickness-dependent interference intensity. Furthermore, the stratified films display a stepwise decrease in thickness over time in conventional interferometry-based measurement of average film thickness, as was first reported[39] by Johonnott (1906). The conventional measurement uses monochromatic laser light and a photodiode for measuring reflected light intensity from a 30−50 μm region[16−18,39] and lacks the spatial resolution necessary for characterizing thickness variations in stratified film along the plane of the film. We recently developed IDIOM (Interferometry Digital Imaging Optical Microscopy) protocols[40−42] with exquisite spatiotemporal resolution (thickness ∼1 nm, in plane < 1 μm, time < 1 ms) for visualizing and analyzing the nanoscopic thickness variations and transitions in stratifying films. In the present contribution, we utilize the IDIOM protocols to obtain AFM-like visualization of topography of ultrathin stratifying foam films (h < 100 nm), as a function of added salt concentration.

The step size obtained from thickness−time plots and from the height difference between distinct, coexisting flat domains are shown to be correlated with the periodicity of supramolecular oscillatory forces,[10,11,16−21,40−44] and the absolute magnitude of their contribution to disjoining pressure can be measured using a thin film balance.[20,42] The step size is also correlated with the interparticle or intermicellar distance. Relatively short-ranged oscillatory structural forces, $\Pi_{os}(h)$, also called hydration or solvation forces, with a period set by the molecular diameter (typically <5 nm), were first detected in simple fluid films confined between two solid substrates using a surface force apparatus (SFA)[1,9,45,46] and were observed in ionic liquids more recently.[47−50] The hydration or solvation forces influence interactions between lipids, proteins, biomacromolecules, and nanoparticles[1,9,51−53] and also lead to stratification or layering during spreading of ultrathin wetting films of simple fluids.[54−57] In multicomponent complex fluids, addition of "smaller" supramolecular structures such as polymers, particles, or micelles at low volume fraction causes the well-known, non-DLVO, depletion interaction,[58−62] which acts to flocculate the "larger" colloidal dispersed objects by an osmotic attraction. However, at relatively high concentration of the "smaller" supramolecular structures, longer ranged, supramolecular oscillatory structural forces (or surface forces) can arise due to confinement-induced layering of micelles,[11,16−21,40−42,63,64] nanoparticles,[16,18,25,26,28−30,65] polyelectrolyte−surfactant complexes,[21,43,44,66−68] bilayers,[69,70] and smectic liquid crystals.[71,72] Even though the influence of supramolecular oscillatory structural forces is most distinctly visualized in stratifying foam films, such forces must arise universally in all multicomponent colloidal dispersions, including foams and emulsions, and influence their stability, lifetime, rheology, and applications.

The present article aims to contribute critical experimental and conceptual advances to address the influence of electrolyte type and concentration on stratification in micellar foam films and is organized as follows. First, we present a comprehensive dataset and discussion of the effect of adding salt on step size and number of steps in micellar foam films. Thereafter we describe a phenomenological model for supramolecular oscillatory structural force that captures the influence of adding surfactant or salt, by including known results for how CMC and aggregation number change on the addition of salt. Our results show that the effect of salt on step size, number of steps, and topography on stratification in freestanding films containing charged micellar systems is fundamentally and strikingly different from the influence of salt on stratifying charged nanoparticle dispersions. Using the IDIOM technique for exquisite thickness determination and topography mapping, we report, recognize, and elucidate the effect of added electrolytes on stratification in micellar foam films. Finally, we show that the influence of salt and surfactant concentration on step size and the number of steps, as well as on the formation of mesas, can be rationalized by examining the concentration-dependent variations in supramolecular oscillatory structural forces using a phenomenological model discussed herein.

RESULTS AND DISCUSSION

Drainage *via* Stratification: Characterization of Stepwise Thinning. Freestanding foam films formed with an aqueous micellar SDS solution (c = 50 mM; c/CMC ≈ 6)

DOI: 10.1021/acsnano.7b05391
ACS Nano 2018, 12, 1050−1061

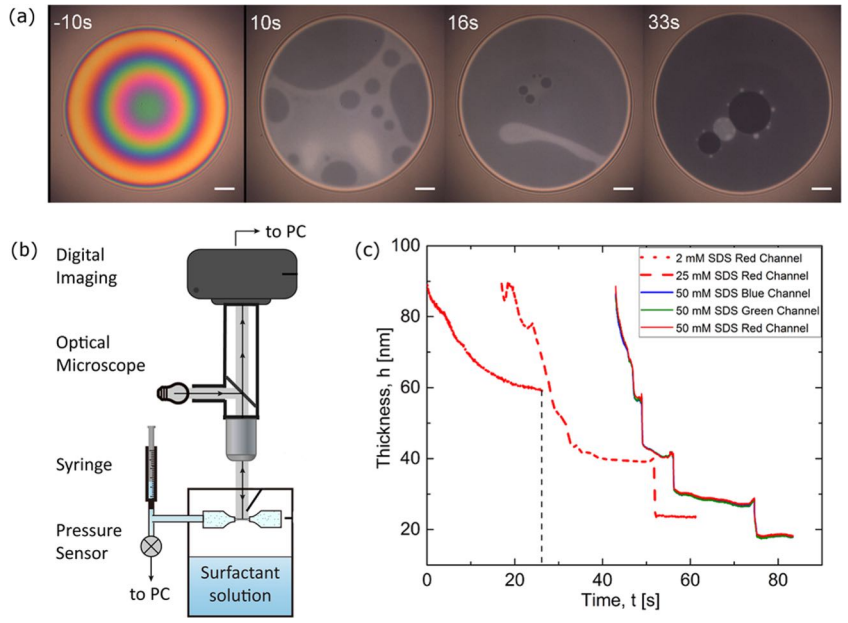

Figure 1. Stratification in sodium dodecyl sulfate (SDS) thin foam films visualized and analyzed using Interferometry Digital Imaging Optical Microscopy (IDIOM) protocols. (a) Snapshots showing drainage *via* stratification in a 50 mM SDS freestanding thin film. Various shades of gray show the coexistence of domains with different thicknesses. The scale bars correspond to 50 μm. (b) Schematic of the IDIOM setup used for visualization and characterization of thickness variations and transitions accompanying drainage *via* stratification. (c) Thickness changes with time computed from a 25 μm side square region at the center of the film contrasted for three different surfactant concentrations. Red, blue, and green lines in 50 mM SDS represent thickness data extracted from the red, green, and blue channels, respectively, of the digital image using the IDIOM protocols. Thickness changes in 2 mM and 25 mM SDS films are shown using only the red channel dataset, and the data are shifted horizontally to show differences in their thinning behavior.

undergo drainage *via* stratification, leading to coexisting regions of discretely different thickness and characteristic stepwise thinning, as shown in Figure 1. Foam films formed in the Scheludko-type cell are visualized and analyzed using IDIOM protocols (see Methods section; schematic in Figure 1b) that rely on computing film thickness from interference intensity. White light reflected from the two air−liquid interfaces of the foam film or soap bubbles with thickness $h > 100$ nm creates brilliant iridescent colors; for thicknesses $h < 100$ nm, progressively thin regions appear as increasingly darker shades of gray (see Figure 1a and movies in the Supporting Information). Regions of different thickness coexist in the stratifying films, and stratification proceeds by spontaneous nucleation and growth of thinner (hence darker) circular domains that grow at the expense of the surrounding thicker film.[18,40,41,63,73] The domain boundaries are sharp, and the expansion of the domains continues until the thickness of the entire film is reduced to the next thickness, smaller by a discrete value equal to the step size.

The progressive thinning of a foam film leads to interference intensity variations, which are analyzed for the quantitative determination of changes in average film thickness for two surfactant concentrations above the CMC and one solution below the CMC (see Figure 1c). The micelle-free foam film made with a 2 mM aqueous SDS solution displays monotonic thinning behavior (CMC of SDS, no added salt, is ∼8.2 mM). In contrast, stepwise thinning is observed in the thickness evolution plots for the micellar SDS foam films with 25 and 50 mM SDS, respectively. For 25 mM SDS foam films, the number of steps is two and the height of each step is $\Delta h = 16.1 \pm 0.5$ nm. On increasing the surfactant concentration to 50 mM, the number of steps increases to four and the height of each step decreases to $\Delta h = 13.5 \pm 0.3$ nm. Each thickness transition is a result of nucleation and growth of thinner (darker) domains driven by the supramolecular oscillatory structural forces that arise due to confinement-induced layering of micelles. The intermicellar spacing that determines the step size decreases as surfactant concentration increases due to the increase in effective screening of electrostatic interactions and additional effects that contribute to the amplitude and frequency of supramolecular oscillatory structural forces, as discussed later.

Intensities corresponding to red, blue, and green channels were analyzed separately, and good agreement is found between thicknesses measured, as is shown for 50 mM SDS. Thus, all channels give similar thickness values.[40,41] Step size and final black film thickness both decrease with an increase in surfactant concentration, whereas the number of steps increases with concentration. The stratification dynamics is visualized for the self-thinning process (volume within the cell is kept constant during drainage), except for $c > 70$ mM salt-free SDS solutions, where the final one or two thickness transitions are induced by increasing capillary pressure (accomplished by changing fluid volume within the fluid cell). Here we focus only on the step size and number of steps and not on the unsteady processes and fluxes governing the transitions. In some studies,[74] the last few thickness transitions are prompted by opening the cell to allow evaporation from the film. Since evaporation changes the relative concentration of surfactant within the solution, making quantitative comparisons difficult, the step size values reported in this study were obtained from a closed cell. We recently showed that IDIOM protocols can be used for creating thickness maps of such stratifying foam films, and the bright halos and white spots observed near the moving front between the expanding domain and surrounding film (in Figure 1a) are due to the formation of nonflat nanoridges and mesas, respectively.[41,42] However, as the plots of average

DOI: 10.1021/acsnano.7b05391
ACS Nano 2018, 12, 1050−1061

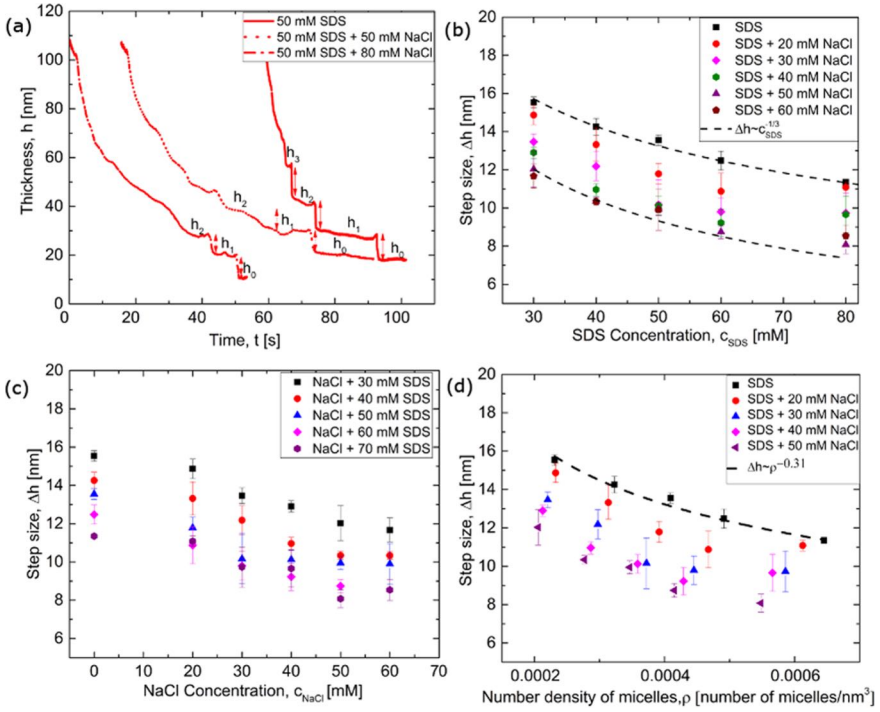

Figure 2. Effect of salt on stratification in aqueous sodium dodecyl sulfate (SDS) thin films. (a) Thickness evolution over time contrasting the stepwise thinning of a salt-free 50 mM SDS solution against 50 mM SDS with 50 mM and 80 mM NaCl added. Increase in salt concentration decreases both the number of steps and the step size. (b) Effect of salt concentration on step size for various SDS concentration thin films: step size decreases both with an increase in surfactant concentration and with an increase in salt concentration. The dotted line shows the concentration-dependent variation in step size $\Delta h \sim c^{-1/3}$ typically associated with stratifying micellar films. (c) Step size variation with increase in salt concentration shown for different SDS concentrations. (d) Step size variations plotted as a function of the number density of micelles showing that the addition of salt reduces the intermicellar distance considerably.

thickness evolution are obtained by averaging intensity from a square region with a 25 μm size (shown in Figure 1c), the appearance of thinner domains, or thicker white spots in the field of view, leads to the observed features in the thickness evolution plots.

Step Size Decreases with an Increase in Surfactant or Salt Concentration. Representative examples of the influence of salt on stepwise thinning are shown in Figure 2, which includes a comparison between salt-free 50 mM SDS and 50 mM SDS with added salt (50 mM and 80 mM NaCl added). Four distinct layers are present in 50 mM SDS, and the height of each step is $\Delta h = 13.5 \pm 0.3$ nm. In contrast, on addition of 50 mM NaCl, the number of steps decreases to three, and the step size decreases to $\Delta h = 9.6 \pm 0.3$ nm. The step size decreases further to $\Delta h \approx 9$ nm on increasing the salt concentration to $c_s = 80$ mM NaCl. Stratification becomes irregular with increasing electrolyte concentration, and layers become difficult to distinguish in the drainage process (see Supporting Information, Figure S3). In the absence of added salt, step size decreases with an increase in surfactant concentration; the concentration-dependence for step size (Δh), thickness of black films (h_0), and their measured values are similar to those reported in the literature.[17,40,41,74−76] The step size Δh is considerably greater than the diameter of the micelles and is also greater than the effective diameter $d = 2(l_{SDS} + \kappa^{-1})$ computed by adding the characteristic size of the counterion atmosphere or screening length represented as Debye length, κ^{-1}, to the micelle size. Here l_{SDS} is the length of SDS molecules;[22] we used $l_{SDS} = 2.3$ nm. An increase in surfactant concentration (and in general, ionic concentration) leads to an increase in screening of electrostatic interactions and a corresponding decrease in Debye length, such that $\kappa^{-1} \propto c^{-1/2}$, as well as a decrease in effective step size. But the experimental results shown in Figure 2 for SDS solutions corroborate that the step size varies with a $\Delta h \propto c^{-1/3}$ power law for micellar solutions with no added salt.

Nikolov *et al.*[16] suggested that the step size is practically equal to the intermicellar distance between the micelles in the bulk and noted that the concentration-dependent variation in step size $\Delta h \propto c^{-1/3}$ is similar to the power law exhibited by confined, ordered latex particles. More recent studies for stratification in spherical nanoparticle dispersions,[26,28,29,31] which include experiments with CP-AFM and X-ray scattering as well as Monte Carlo simulations, reveal that the step size depends only on the particle number density ρ ($\Delta h \propto \rho^{-1/3}$) and not on the effective particle diameter $2(R + \kappa^{-1})$. As the addition of salt or electrolyte does not change the particle size and number density, the step size does not change with the electrolyte concentration for films containing nanoparticles. However, the magnitude (or amplitude) of the disjoining pressure and decay length (or correlation length) measured using CP-AFM shows a distinct dependence on the electrolyte concentration.[26,77] The amplitude decreases with an increase in salt concentration, implying stepwise transitions require a lower energy barrier and become more likely to occur.[26,77]

Danov *et al.*[22] and Anachkov *et al.*,[74] who utilized experimental datasets acquired for salt-free micellar solutions and three different theoretical approaches to account for intermicellar interactions, determined that the step size depends primarily on micelle number density, $\Delta h \propto \rho^{-1/3}$,

DOI: 10.1021/acsnano.7b05391
ACS Nano 2018, 12, 1050−1061

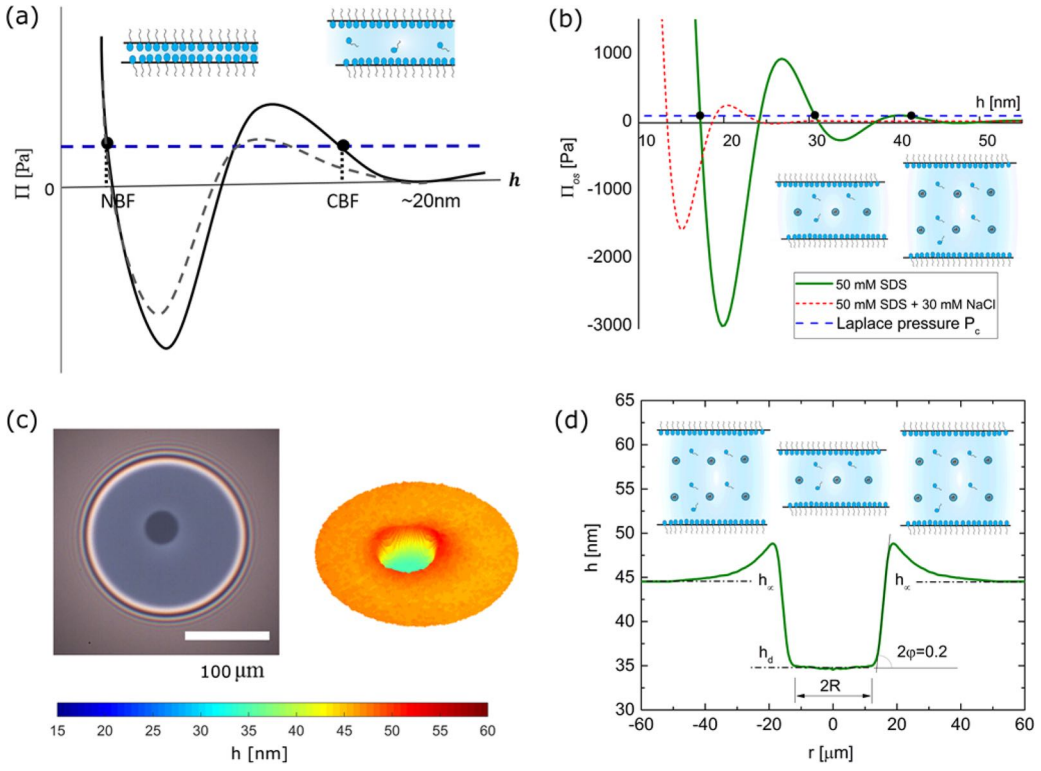

Figure 3. Thickness transitions within foam films made with ionic surfactants are determined by the interplay of disjoining pressure and Laplace pressure. (a) Disjoining pressure curves for foam films made with ionic surfactants, showing contrast between solutions with (solid) and without (dotted) added salt. The disjoining pressure for two thicknesses (CB and NB, shown schematically, for thicknesses corresponding to the filled dots) counterbalances the capillary pressure. (b) Supramolecular oscillatory structural force contribution to disjoining pressure provides multiple thicknesses that can counterbalance an applied capillary pressure. The influence of adding surfactant or salt is captured by the phenomenological model discussed in the text. The three filled dots on the curve for a 50 mM SDS solution represent the three metastable thicknesses predicted for an applied Laplace pressure, P_c. (c) Gray-scale image showing a thinner darker domain, with its thicker surrounding. The accompanying thickness map, obtained using IDIOM protocols and shown here with an oblique perspective, highlights the nonflat transition region and the relatively uniform thickness in the flat regions. (d) Experimentally determined thickness profile showing the shape of the nanoridge as well as the size of the thinner domain region. The schematics illustrate the layered structure of micelles within the flat regions of the film. The nanoridge is relatively flat (the height is shown in nm scale, whereas the lateral dimension is in μm scale), and the contact angle is relatively small. The intermicellar distance determines the step size and is itself quite sensitive to the concentration of added salt.

and not on the effective micelle diameter, in analogy with the observations for nanoparticle dispersions. Furthermore, Anachkov *et al.*[74] argued that the concentration-dependent step size can be used to analyze micelle size, aggregation number, and charge, but all the comparisons were carried out for surfactant solutions with low or no added salt. Increase in surfactant concentration increases the number density of micelles, $\rho = (c - \mathrm{CMC}) \times N_A/N_{agg}$, but the aggregation number (number of surfactant molecules self-assembled per micelle) also increases with surfactant concentration. Bales and Almgren[78] showed that the aggregation number of SDS micelles increases as the one-fourth power of total surfactant concentration, implying that as the concentration of surfactant increases, the number density itself increases by 3/4 power. However, as the surfactants formed spherical micelles only for a limited range of concentrations, experimental data can be fit equally well by the two correlations $\Delta h \propto c^{-1/3}$ and $\Delta h \propto \rho^{-1/3}$, as has been observed for surfactant solutions.

For a fixed concentration of surfactant, the increase in salt concentration also leads to a decrease in step size, and Figure 2b illustrates these changes for five different concentrations of added surfactant. Although decrease in step size with increasing surfactant concentration has been reported before, Figure 2b shows the first systematic examination of the influence of added salt on stratifying micellar films. The effect of added electrolyte (NaCl; 1 mM < c_s < 60 mM) is quantified in terms of change in the number and the size of steps and by visualizing topographical changes, as discussed in the following section. Addition of salt leads to a lowering of critical micelle concentration as well as an increase in aggregation number, and hence the number density of micelles is itself sensitive to added salt. However, the plot of step size as a function of salt concentration (Figure 2c) for fixed surfactant concentration, as well as the step size variation with the number density of micelles (see Figure 2d), show strong dependence on added electrolyte concentration to Figure 2b. In contrast with nanoparticle dispersions, the shape and size of ionic spherical micelles, as well as electrostatic interactions between them, are sensitive to the presence of electrolyte. Decrease in the layer spacing (or step size) on addition of salt shows that screening of electrostatic interactions and decrease in Debye length play a significant role, in addition to the role played by increase in the number density of micelles. Using light scattering, Krichevsky and Stavans[79,80] observed a similar decrease in step size for three concentrations of added salt, for relatively high concentrations of SDS (8% by weight or ~280 mM) in

DOI: 10.1021/acsnano.7b05391
ACS Nano 2018, 12, 1050−1061

glycerol/water mixtures. Likewise, Tabor *et al.*[64] reported a decrease in step size on adding salt for 200 mM SDS solutions using AFM and neutron scattering data. Although we restricted our studies to concentrations below 100 mM SDS to minimize the influence of size and shape polydispersity, both the scattering studies support trends highlighted in our study. In the next section, we scrutinize the role of different parameters by relying on a phenomenological model for calculating and incorporating the effect of added salt and surfactant on the amplitude and periodicity of the supramolecular oscillatory structural forces.

Supramolecular Oscillatory Structural Force Contribution to Disjoining Pressure. In micelle-free foam films, the combined influence of three primary contributions[10,81,82]—attractive dispersion $\Pi_{vw}(h)$, repulsive, electrostatic double layer forces, $\Pi_{el}(h)$, and shorter ranged, solvation, or steric forces—leads to a nonmonotonic disjoining pressure curve, as shown in Figure 3a. The disjoining pressure can counterbalance the capillary pressure for two distinct thicknesses, known as thicker "common black" or thinner "Newton black" film ($h \approx$ few nm). Although we have invoked the mechanical definition for $\Pi(h)$ in the discussion so far, thermodynamically, disjoining pressure represents the work required to reduce the thickness of a film at constant pressure (P), temperature (T), surface area (A), and the mole number of species (N_i). Disjoining pressure is an intensive property, and variation in disjoining pressure can drive fluxes in analogy with how changes in entropy, chemical potential, or pressure drive transport. Thus, the disjoining pressure can be defined in terms of the Gibbs free energy, G, as

$$\Pi(h) = -\left(\frac{\partial G}{\partial h}\right)_{T,P,A,N_i} \tag{1}$$

The nonmonotonic shape of the thickness-dependent disjoining pressure curve is quite analogous to the pressure−volume isotherm for real gases.[81,82] The $P-V$ diagrams can be analyzed to show the coexistence of liquid and gas phases, and likewise in foam films, thermodynamically, a phase transition *via* nucleation and growth leads to formation of Newton black film (or to the coexistence of two blacks). Furthermore, the nonmonotonic, stepwise thinning[10,16−20] and coexistence of thick and thin films in stratifying micellar foam films are a consequence of the role played by non-DLVO, supramolecular oscillatory structural forces.[10,19−22] Thus, the successive layers with a quantized difference in thickness of flat regions correspond to a sequence of metastable thicknesses, and the spontaneous emergence of thinner darker domains occurs by nucleation and growth. In Figure 3b, the three thicknesses in metastable equilibrium with an imposed Laplace pressure are shown for 50 mM SDS solutions with dark, filled dots. The change in both amplitude and frequency of oscillations on addition of salt shifts the disjoining pressure curve, leading to a reduction in both the activation energy for nucleation and growth of thinner layers and a reduction in the number of layers (as shown in Figure 3b, and a discussion of the model used for supramolecular oscillatory structural forces follows next).

For micelle-free films formed by SDS concentrations below the CMC value, the addition of salt results in progressive screening of electrostatic interactions, and for these films, the equilibrium thickness of "common black films" decreases as the salt concentration is increased, in accordance with the DLVO theory.[83] However, at relatively high concentrations of salt, DLVO theory is no longer applicable, and eventually much thinner "Newton black films" form, which contain only a hydration layer.[83,84] Likewise, in the micellar systems, the electrostatic repulsion between head-groups of the surfactant is progressively screened on addition of salt, resulting in the lowering of the critical micelle concentration, and shorter Debye length. However, at the same time, the adsorption at the liquid−air interface also becomes more pronounced on addition of salt, leading to a lower surface tension, which results in a lower capillary pressure (assuming the film size is kept constant). As the surface tension above the CMC exhibits nearly a concentration-independent value for micellar solutions, the observed changes in stratification kinetics and dynamics must be solely driven by a change in disjoining pressure. Although the nucleation of thinner darker domains is energetically favored, and the domains are indeed a step size thinner than the flat surrounding films, due to local conservation of mass, the fluid displaced from the thinner domain forms a shallow ridge near the contact line. The width of the ridge is in micrometers, even though its height is in nanometers (see Figure 3c,d). Therefore, the transition from n to $n-1$ layers occurs nearly seamlessly over a wide region while keeping the micelle shape and size intact. The intermicellar spacing obtained from neutron scattering, AFM, simulations, and stratified micellar thin films is shown to agree,[41,64,65,76,79,80] and this suggests that micelles (like nanoparticles) preserve their size, shape, and number density during stratification. Indeed, we have recently shown[42] that the shape and shape evolution of the ridge can be quantitatively described using the thin film equation, augmented with a contribution by supramolecular structural forces, and comparison of experiments and theory shows the viscosity of micellar solutions in confined films is similar to their shear viscosity obtained from measurements using torsional rheometry.

The simplest estimate for supramolecular oscillatory structural forces can be made by using an approximate expression, $\Pi_{os} = kT\rho \cos(2\pi h/d) \exp(-h/d)$, based on an expression often used for hydration or solvation forces.[1] Here both the oscillatory wavelength (which determines the step size) and the decay length (which determines the number of layers) are set to be equal to particle size, d, and ρ represents the bulk particle number density. We follow the framework developed by Kralchevsky and Denkov,[22] but we have modified the approximate phenomenological expressions to elucidate how concentration of surfactant and salt influence the magnitude and decay length of the supramolecular oscillatory surface forces.

$$\Pi_{os} = \frac{(c - \mathrm{cmc})N_A}{N_{agg}} f(\varphi) k_B T \cos\left(\frac{2\pi h}{\Delta h}\right) \exp\left[\left(\left(\frac{d}{\Delta h}\right)^3 - \frac{h}{\Delta h}\right) g(\varphi)\right] \tag{1a}$$

$$f(\varphi) = \frac{(1 + \varphi + \varphi^2 - \varphi^3)}{(1-\varphi)^3};$$
$$g(\varphi) = \frac{\sqrt{2/3} + a_1\Delta\varphi + a_2(\Delta\varphi)^2}{(b_1/\Delta\varphi) - b_2} \tag{1b}$$

Here, the prefactor explicitly shows the dependence on surfactant concentration, critical micelle concentration, aggregation number, temperature, and volume fraction and includes a compressibility factor derived by Carnahan and Starling for

DOI: 10.1021/acsnano.7b05391
ACS Nano 2018, 12, 1050−1061

Table 1. Characteristic Values of the Effective Volume Fraction, Computed Debye Length, Estimate for Compressibility Factor, Estimate for Geometric Factor, and the Measured Values of Step Size

c_{SDS} [mM]	c_{NaCl} [mM]	Δh [nm]	κ^{-1} [nm]	d [nm]	N_{agg} [−]	φ [−]	ρ [no. of micelles/nm^3]	$f(\varphi)$ [−]	$g(\varphi)$ [−]
30	0	15.3	2.86	10.3	56.5	0.13	2.31×10^{-04}	1.76	3.14
50	0	13.8	2.57	9.7	61.3	0.20	4.09×10^{-04}	2.38	2.38
100	0	10.3	2.11	8.8	69.9	0.28	7.89×10^{-04}	3.64	1.64
30	50	12.1	1.28	7.2	81.1	0.04	2.06×10^{-04}	1.18	4.72
50	50	9.6	1.25	7.1	82.9	0.06	3.47×10^{-04}	1.31	4.22
100	50	8.5	1.18	6.9	86.9	0.12	6.77×10^{-04}	1.66	3.32

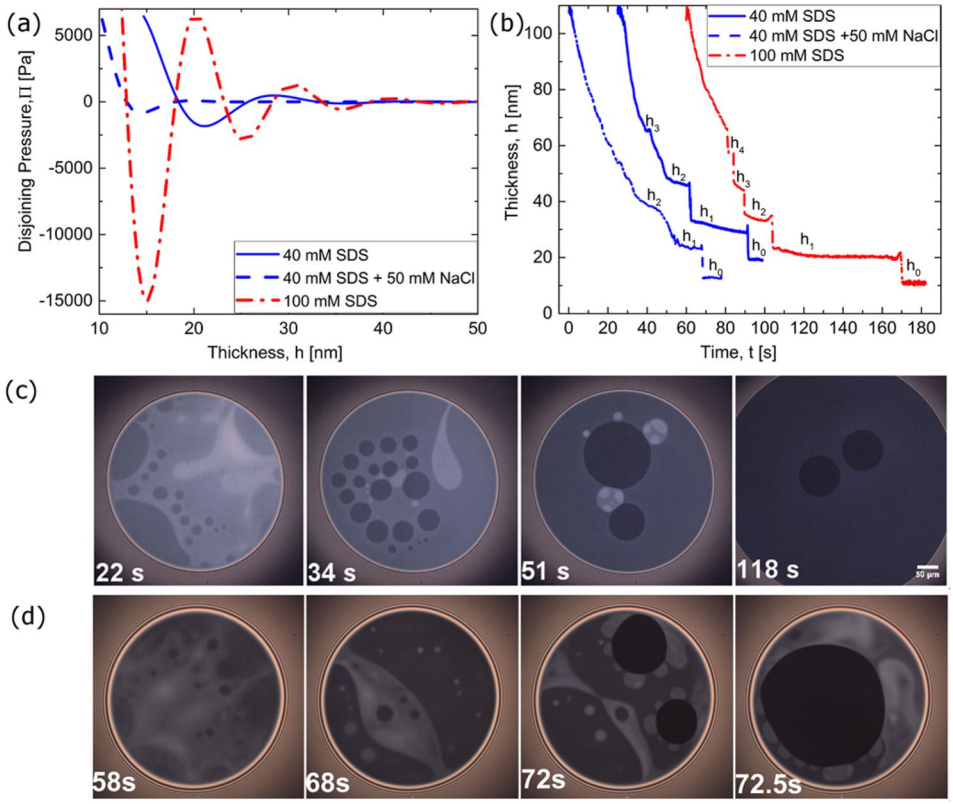

Figure 4. Contrasting the effects of increasing the surfactant concentration against an increase in salt concentration. (a) Disjoining pressure variation for 40 mM SDS solution contrasted with 100 mM SDS and 40 mM SDS with 50 mM salt added. Even though 100 mM SDS and 40 mM SDS with salt added have the same periodicity, the model calculations show that the number of layers increases with an increase in surfactant concentration, whereas the decay length and amplitude decrease with addition of salt. (b) Both step size and final thickness decrease with addition of surfactant and salt, but the number of steps decreases with added salt, whereas the number of steps increases on addition of surfactant (contrast 100 mM SDS with 40 mM SDS), as predicted by the model (see text for details). (c) Sequence of images showing the thickness variations in a stratifying 100 mM SDS solution. (d) Image sequence showing that the thickness variations in a stratifying 40 mM SDS solution with 50 mM salt are quite distinct from observations for all micellar SDS solutions (25 mM < c < 100 mM) investigated. At 68 s, many isolated white spots or mesas appear in micellar film with added salt, and at 72 s, relatively large radii mesas flanking the expanding darker domain can be observed. The model calculations show that the amplitude of disjoining pressure decreases on adding salt, leading to an increase in the number and size of white spots spontaneously formed in stratifying micellar films.

hard spheres.[85] The number density of the micelles is given by $\rho = (c - \mathrm{cmc})N_A/N_{agg}$, the effective volume fraction, φ, of the micelles is defined as $\varphi = \rho\pi d^3/6$, and the parameters $\Delta\varphi = \pi/3\sqrt{2} - \varphi$ and the values for $a_1 = 0.24$, $a_2 = 0.63$, $b_1 = 0.49$, and $b_2 = 0.42$ are based on the formulas and values determined by Kralchevsky and Denkov.[86] The representative values of all the computed parameters (see discussion that follows) are shown in Table 1.

The modified calculation of the supramolecular oscillatory structural force involves (a) equating the experimentally measured step size with the oscillation wavelength, as the oscillatory nature of the disjoining pressure is captured by the cosine term; (b) evaluating a concentration-dependent effective size using $d = 2(R + \kappa^{-1})$, where the Debye length is estimated using $\kappa^2 = 8\pi l_B[\mathrm{CMC} + \alpha(c - \mathrm{CMC})]$, where α is the degree of ionization, and the Bjerrum length $l_B = e^2/\varepsilon kT = 0.72$ nm for water; (c) estimating the amplitude, $\rho f(\varphi)kT$, using the compressibility factor $f(\varphi)$ (rewritten based on original expressions provided by Kralchevsky and Denkov[86]); and (d) estimating the decay length $\Delta h/g(\varphi)$, which depends on the effective volume fraction as well as the step size, and the geometric factor $g(\varphi)$, determined from Henderson's theory.[87] The exponential term accounts for the diminishing effect of confinement with distance. Our calculations show that the decay length increases with concentration of the surfactant, even though both step size and $g(\varphi)$ decrease, in agreement

DOI: 10.1021/acsnano.7b05391
ACS Nano 2018, 12, 1050−1061

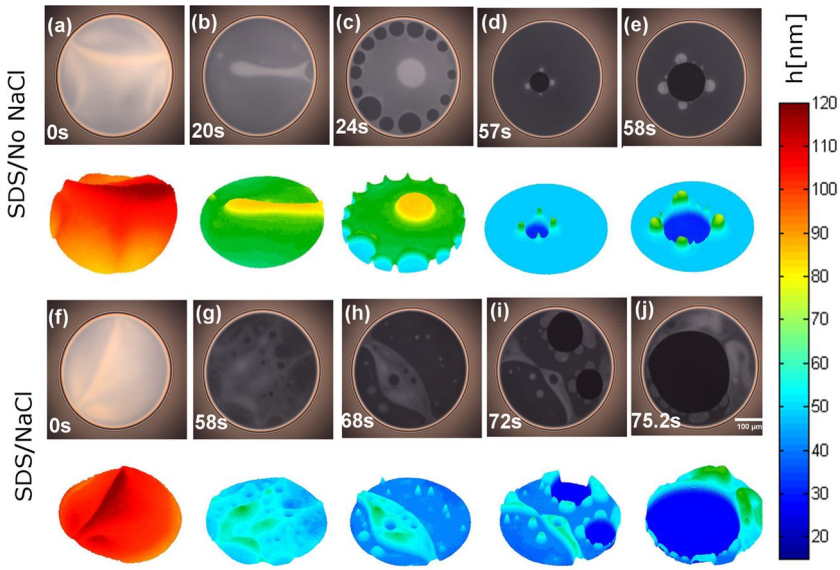

Figure 5. Effect of added salt on topographical features and transitions in a stratifying film. Snapshots from (a) to (e) in multiple shades of gray represent the stratification process for 40 mM SDS thin films as visualized using the IDIOM setup. Stratification process for SDS solutions with added salt (NaCl), added SDS, and salt-free SDS thin films and the corresponding height maps extracted using the IDIOM protocols. The height maps show the coexistence of different thicknesses. Snapshots from (f) to (j) show the stratification process for 40 mM SDS + 50 mM NaCl. Addition of salt increases the size of mesas formed around the expanding domains and also increases the overall number of mesas. The scale bar corresponds to 50 μm. The height of the mesas is shown in nm scale, whereas the lateral dimension is in μm scale.

with the experiments. The estimate for the Debye length includes an explicit dependence on the concentration (or number density) of charged micelles and accounts for the reduction in fluid volume available to counterions due to the presence of micelles,[22,74] in analogy with the Debye length estimates included in many studies that describe behavior of charged spheres undergoing order−disorder transitions at relatively low volume fractions.[88−91]

A representative example shown in Figure 4a contrasts the theoretical estimate for supramolecular oscillatory structural force contributions to disjoining pressure for three solutions: 40 mM SDS solution, 100 mM SDS solutions, and 40 mM SDS with 50 mM salt added. Although the latter two solutions have similar step size, the model calculations show that the disjoining pressure isotherms are strikingly different. The plots in Figure 4a (and the data in Table 1) show that in salt-free solutions an increase in surfactant concentration leads to a substantial increase in the amplitude or prefactor $(\rho f(\varphi)kT)$, increase in decay length, and a decrease in step size, and hence the total number of steps increases. However, if salt is added at a fixed surfactant concentration, the decrease in CMC value as well as Debye length contributes to a substantial reduction in decay length and amplitude of the disjoining pressure, as shown in Figure 4a and Table 1. Experimental results on the stepwise thinning shown for the three solutions agree remarkably well with the theoretical predictions in terms of the change in the number of steps on adding either salt or surfactant. Four distinct layers can be discerned in stratifying films of 40 mM SDS with the step size Δh = 14.2 ± 0.4 nm. In contrast, on addition of 50 mM NaCl, the number of steps or layers decreases to three, and the step size decreases to Δh = 10.3 ± 0.3 nm. In comparison, five distinct layers appear in stratifying films of 100 mM SDS with the step size Δh = 10.3 ± 0.4 nm.

For a fixed low salt concentration or for a salt-free solution, an increase in surfactant concentration that leads to an increase in the amplitude or prefactor $(\rho f(\varphi)kT)$ is responsible for a higher stability against drainage manifested by SDS solutions with higher concentration (higher capillary pressures needed to reach the last stage of thinning for >70 mM solutions). Furthermore, an increase in surfactant concentration leads to a decrease in the effective size and Debye length, and therefore a decrease in the wavelength that corresponds to a decrease in step size. Lastly in the salt-free solutions, an increase in surfactant concentration leads to an increase in decay length $(\Delta h/g(\varphi))$, leading to the observed increase in the number of layers. However, for a fixed surfactant concentration, the addition of electrolyte decreases the CMC value and increases the aggregation number, and both together affect the size and the number density of micelles and hence the wavelength and amplitude of the supramolecular oscillatory structure forces. Furthermore, the amplitude, wavelength, and decay length all decrease with an increase in salt concentration, leading to a decrease in step size as well as a decrease in number of layers. As the amplitude of the oscillatory forces is dampened by the addition of salt, the stepwise transitions are facilitated, and in Figure 4c,d, we show a few representative snapshots of stratified films. A decrease in the amplitude enhances the formation of white spots that emerge near the moving front between the expanding domain and its surrounding and likewise also increases the number of white spots that spontaneously emerge, as discussed in next section.

Addition of Salt Modifies the Topography of Stratifying Foam Films. Comparison between 40 mM SDS solutions with no salt added and an SDS/NaCl mixture (40 mM SDS with 50 mM NaCl) on the stratification process is shown in Figure 5, where thickness differences are emphasized in the thickness maps created using IDIOM protocols. As the array of photodiodes in the digital camera simultaneously record pixelwise intensity maps for three wavelengths (red, green, and blue), we show that it is possible to create thickness maps with nanoscopic thickness resolution, whereas the in-plane resolution is comparable to optical microscopy.[40,41] The

DOI: 10.1021/acsnano.7b05391
ACS Nano 2018, 12, 1050−1061

stratification process in a 40 mM SDS thin film is shown in snapshots from (a) to (e). Furthermore, the snapshots from (f) to (j) correspond to the mixture of 40 mM SDS and 50 mM NaCl. The effect of added salt on the stratification process is also manifested in the shape and size of the white spots. The thickness mapping using IDIOM protocols shows that these white spots are thicker than the surrounding darker film and have relatively flat tops (hence we call them mesas). As the height of the mesas is shown in nanometer scale, the lateral dimension is in 1000 nm (in μm) scale; realistically these mesas are like pancakes with a thickness almost 2 orders of magnitude smaller than the diameter. The mesas flanking an expanding domain in stratifying films containing SDS/NaCl mixtures are larger in size and thinner in comparison to SDS foam films. Furthermore, multiple isolated white spots or mesas spontaneously emerge in stratifying films containing added salt. All the published studies on SDS/NaCl mixtures focused on suppression of stratification on the addition of salt; however the topography in the SDS/NaCl mixture foam films have not been reported and analyzed before.

Zhang and Sharma[40] showed two distinct regimes of domain expansion dynamics in SDS foam films: isolated domains display a diffusive growth law $R \propto t^{1/2}$, and a second regime with $R \propto t$ scaling is exhibited after domains coalesce with the Plateau border or after an instability creates mesas at the moving edge between the expanding domain and its thicker surroundings. However, on the addition of salt, the foam films rarely show a diffusive growth regime for isolated domains. Furthermore, Zhang and Sharma[42] recently showed that the shape of the nonflat regions such as mesas and ridges depends on the interplay of thickness-dependent disjoining pressure and curvature-dependent capillary pressure. As the magnitude of surface tension as well as disjoining pressure decreases upon the addition of salt, the nonflat features appear more readily, and very large mesas can be observed in thickness maps created using IDIOM. An examination of the disjoining pressure isotherm (Figure 4a) shows that a lower amplitude (or prefactor) makes the system more susceptible to instability, and therefore relatively large mesas form, as observed. In addition to the mesas formed at the moving front between the expanding domain and its thicker surroundings, the addition of salt promotes the nucleation and growth of isolated mesas. Such isolated mesas are rarely seen in nearly salt-free SDS solutions.

The nucleation and growth of isolated thicker mesas, as well as of thinner domains (and the nanoridges around them), is driven by the oscillatory nature of disjoining pressure. An oscillatory disjoining pressure implies that the free energy functional, $G(h)$ (using $\Pi = \partial G/\partial h$), is also oscillatory, and the number of oscillations is determined by the decay length. In analogy with binary systems that phase separate[2] when their concentration-dependent free energy has two minima and one maxima at an intermediate concentration (typical for Flory–Huggins theory for polymer blends for example), ultathin films appear to separate into thicker and thinner regions. For metastable binary systems that phase separate by a nucleation and growth mechanism, the final outcome is drops rich in phase A dispersed in the matrix of B or *vice versa* (depending upon the initial composition). Likewise, the metastable thin films can nucleate and grow either thicker mesas or thinner domains, as observed here.

CONCLUSIONS

In this study, we utilize experiments carried out in a Scheludko-like cell and a phenomenological model for supramolecular oscillatory structural forces to elucidate how the addition of surfactant or salt affects stratification in micellar foam films. We find that an increase in concentration of either salt or surfactant leads to a decrease in step size. However, although the number of steps increases with an increase in surfactant concentration, the number of steps decreases with an increase in the concentration of added salt. We show that the thermodynamics underlying the coexistence of thick–thin regions and thickness variations and transitions in stratifying foam films can be described nearly quantitatively by a phenomenological model for supramolecular oscillatory structure force contribution to the disjoining pressure (see eq 1, Table 1, and the related discussion). Calculations described herein show that the decay length and amplitude of the supramolecular oscillatory structural forces both increase with the addition of surfactant in salt-free solutions. In contrast, the addition of salt results in a decrease in both amplitude and decay length, resulting in fewer stepwise thinning transitions, as can be observed for SDS solutions with added salt, in agreement with the model calculations. Although many studies emphasize the similarity between the stratification due to micelles and nanoparticles, we find that the step size decreases on addition of salt for micellar systems, in contrast to a constant value obtained for charged nanoparticle systems. We argue that the overall effect of adding salt is more dramatic for micellar systems, as both the number density and the effective size of micelles (determined by both Debye length and aggregation number) change on addition of salt, contrastingly neither the number density nor the actual size of nanoparticles changes on addition of salts.

The thickness-dependent supramolecular oscillatory structural forces drive the formation of coexisting thick and thin flat regions, as well as the emergence of nonflat structures such as nanoridges and mesas that spontaneously form during drainage of stratifying, micellar freestanding films. The phenomenological model accounts for how changes in the effective micelle size (computed by incorporating concentration-dependent variation in Debye length), critical micelle concentration, aggregation number, and effective number density of micelles influence the supramolecular structural forces. The influence of added salt on thickness variations in micellar freestanding films is visualized and analyzed in this study using IDIOM protocols with exquisite spatial (thickness <10 nm, lateral ~500 nm) and temporal resolution (<1 ms). As the magnitude of surface tension as well as of disjoining pressure decreases upon the addition of salt, the nonflat ridges and mesas appear more readily. Relatively large mesas can be observed in the presence of salt in the thickness maps of stratifying films. In addition to the mesas that form at the moving front between expanding domain and its thicker surroundings, the addition of salt promotes the nucleation and growth of isolated mesas. Such isoltaed mesas are rarely seen in nearly salt-free SDS solutions. In this study, we restricted the study to intermediate salt concentrations (1 mM < c_s < 60 mM), and aqueous solutions of anionic surfactant (SDS) form spherical micelles for such salt concentrations, typically found in water from natural resources. We anticipate the findings from the current study will enable a better understanding of how different surfactants behave when the ionic content or hardness of water is varied and in the design of foams with better control over their stability. Lastly,

DOI: 10.1021/acsnano.7b05391
ACS Nano 2018, 12, 1050–1061

we anticipate that our comprehensive experimental data, our technique for visualizing and analyzing thickness transitions and variations, and the phenomenological model for supramolecular surface forces included here will drive the future progress in this field.

MATERIALS AND METHODS

Materials: Aqueous SDS Solution with and without Added Salt (Sodium Chloride). Horizontal foam films are formed with a mixture of an ionic surfactant (SDS) and sodium chloride (NaCl) all at room temperature above the critical micelle concentration. SDS (anionic surfactant, molecular weight of 288.38 Da, Sigma-Aldrich Co., St. Louis, MO, USA, L6026, >99.0%) is used without purification. NaCl (molecular weight of 58.5 Da, Sigma-Aldrich, Co., S9888, ≥99.0%) was used as received. All of the solutions are prepared with deionized water with a resistivity of 18.2 Ω. The critical micelle concentration of pure SDS is 8.3 mM at 25 °C, and it decreases with addition of NaCl. CMC decreases with increasing salt concentration, and the aggregation number increases with increasing salt concentration. Both the surfactant and salt concentrations are below 100 mM.

Thin Film Thickness Measurement Using Interferometry Digital Imaging Optical Microscopy. Drainage and stratification experiments are conducted using a Scheludko-like thin film cell that consists of a glass tube, with a side arm attached to a syringe pump. A biconcave drop is formed within the cell by slowly withdrawing liquid using a syringe pump to form a plane-parallel film with desired size and initial thickness (<100 nm), surrounded on all sides by a thicker meniscus (that emulates a Plateau border). As the capillary pressure depends upon both the film size and the cell size, the sizes are kept similar for all stratification experiments to have a meaningful comparison.[5] The thin film is illuminated by white light, and the intensity variations within the stratifying thin film drainage are recorded with a FASTCAM Mini UX 100 high speed camera attached to a magnification system (Navitar Zoom 6000, with added microscope objective) (Figure 1b). Every pixel in a color image obtained by a digital camera can be read as a composite of three intensities of red (wavelength λ = 650 nm), green (λ = 546 nm), and blue (λ = 470 nm) light, and each color channel has values in the range of 0−4095 (for a RAW image with a 12-bit depth). The IDIOM protocols rely on white light illumination and use digital filtering to obtain simultaneous intensity maps and consequently thickness measurements by using the interferometry equation

$$h = \left(\frac{\lambda}{2n\pi}\right) \arcsin\left(\sqrt{\frac{\Delta}{1 + 4R(1 - \Delta)/(1 - R)^2}}\right) \quad (2)$$

where λ is the wavelength of light, $\Delta = (I - I_{min})/(I_{max} - I_{min})$, and $R = (n - 1)^2/(n + 1)^2$. Here I is the intensity value measured in each pixel, I_{max} and I_{min} are the maximum and minimum intensity values, and n is the refractive index of the bulk solution (here n = 1.33). The Fresnel coefficient $R = (n - 1)^2/(n + 1)^2$ is computed by using the refractive index n of the bulk solution (in this case, we assume n = 1.33). The image analysis is carried out in MATLAB R2015a with specially developed codes. With the aforementioned microscope assembly, the thickness measurement reaches a spatial resolution of 0.5 μm/pixel, thickness resolution of ∼1 nm, and under a millisecond temporal resolution, as detailed in our earlier contributions.[40−42] Recently, Beltramo and Vermant[92] adopted our methodology for visualization and analysis of lipid films and obtained even finer thickness resolution by using a 16-bit camera (we use 12-bit raw images).

ASSOCIATED CONTENT

Supporting Information

The Supporting Information is available free of charge on the ACS Publications website at DOI: 10.1021/acsnano.7b05391.

Plot of surface tension as a function of surfactant concentration for various salt concentrations and additional stepwise thickness evolution profiles (PDF)

Movies visualizing stratification in freestanding foam films formed with salt-free and salt-added aqueous micellar SDS solution and a movie showing thickness maps created using IDIOM protocols (AVI)

(AVI)

(AVI)

(AVI)

AUTHOR INFORMATION

Corresponding Author

*viveks@uic.edu

ORCID

Vivek Sharma: 0000-0003-1152-1285

Notes

The authors declare no competing financial interest.

ACKNOWLEDGMENTS

V.S. would like to acknowledge funding support by the College of Engineering and the Department of Chemical Engineering at University of Illinois at Chicago. The students (S.Y. and Y.Z.) were supported by start-up funds as well as funding by the Campus Research Board. V.S. also acknowledges funding for his Mentored Professional Development Program initiative, which was responsible for motivating a former undergraduate researcher (R.R.) to carry out experiments included in this article. V.S. thanks Cynthia Jamieson, UIC, and the reviewers for close reading of the manuscript and insightful questions and comments. Y.Z. is currently a postdoctoral research associate in Chemical Engineering, University of California at Berkeley.

REFERENCES

(1) Israelachvili, J. N. *Intermolecular and Surface Forces*, 3rd ed.; Academic Press, 2011.

(2) Fennell Evans, D.; Wennerström, H. *The Colloidal Domain: Where Physics, Chemistry, Biology, and Technology Meet*, 2nd ed.; Wiley-VCH: New York, 1999.

(3) Derjaguin, B. V.; Churaev, N. V.; Muller, V. M. *Surface Forces*; Springer: New York, 1987.

(4) Derjaguin, B. V.; Titijevskaia, A. S.; Abricossova, I. I.; Malkina, A. D. Investigations of the Forces of Interaction of Surfaces in Different Media and Their Application to the Problem of Colloid Stability. *Discuss. Faraday Soc.* **1954**, *18*, 24−41.

(5) Sheludko, A. Thin Liquid Films. *Adv. Colloid Interface Sci.* **1967**, *1*, 391−464.

(6) Vrij, A. Possible Mechanism for Spontaneous Rupture of Thin Free Liquid Films. *Discuss. Faraday Soc.* **1966**, *42*, 23−33.

(7) Mysels, K. J.; Jones, M. N. Direct Measurement of the Variation of Double-Layer Repulsion with Distance. *Discuss. Faraday Soc.* **1966**, *42*, 42−50.

(8) Gochev, G.; Platikanov, D.; Miller, R. Chronicles of Foam Films. *Adv. Colloid Interface Sci.* **2016**, *233*, 115−125.

(9) Israelachvili, J.; Ruths, M. Brief History of Intermolecular and Intersurface Forces in Complex Fluid Systems. *Langmuir* **2013**, *29*, 9605−9619.

(10) Bergeron, V. Forces and Structure in Thin Liquid Soap Films. *J. Phys.: Condens. Matter* **1999**, *11*, R215−R238.

(11) Langevin, D.; Sonin, A. A. Thinning of Soap Films. *Adv. Colloid Interface Sci.* **1994**, *51*, 1−27.

(12) Blossey, R. *Thin Liquid Films: Dewetting and Polymer Flow*; Springer, 2012.

DOI: 10.1021/acsnano.7b05391
ACS Nano 2018, 12, 1050−1061

(13) Kalliadasis, S.; Thiele, U. *Thin Films of Soft Matter*; SpringerWien: NewYork, 2007.
(14) Mukherjee, R.; Sharma, A. Instability, Self-Organization and Pattern Formation in Thin Soft Films. *Soft Matter* **2015**, *11*, 8717−8740.
(15) Seemann, R.; Herminghaus, S.; Neto, C.; Schlagowski, S.; Podzimek, D.; Konrad, R.; Mantz, H.; Jacobs, K. Dynamics and Structure Formation in Thin Polymer Melt Films. *J. Phys.: Condens. Matter* **2005**, *17*, S267.
(16) Nikolov, A. D.; Wasan, D. T. Ordered Micelle Structuring in Thin Films Formed from Anionic Surfactant Solutions: I. Experimental. *J. Colloid Interface Sci.* **1989**, *133*, 1−12.
(17) Nikolov, A. D.; Kralchevsky, P. A.; Ivanov, I. B.; Wasan, D. T. Ordered Micelle Structuring in Thin Films Formed from Anionic Surfactant Solutions: Ii. Model Development. *J. Colloid Interface Sci.* **1989**, *133*, 13−22.
(18) Nikolov, A. D.; Wasan, D. T.; Kralchevsky, P. A.; Ivanov, I. B. In *Ordered Structures in Thinning Micellar Foam and Latex Films*, Ordering and Organisation in Ionic Solutions, Kyoto, Japan; Sogami, N. I. a. I., Ed.; World Scientific, Singapore: Kyoto, Japan, 1988; pp 302−414.
(19) Bergeron, V.; Jimenez-Laguna, A. I.; Radke, C. J. Hole Formation and Sheeting in the Drainage of Thin Liquid Films. *Langmuir* **1992**, *8*, 3027−3032.
(20) Bergeron, V.; Radke, C. J. Equilibrium Measurements of Oscillatory Disjoining Pressures in Aqueous Foam Films. *Langmuir* **1992**, *8*, 3020−3026.
(21) Bergeron, V.; Langevin, D.; Asnacios, A. Thin-Film Forces in Foam Films Containing Anionic Polyelectrolyte and Charged Surfactants. *Langmuir* **1996**, *12*, 1550−1556.
(22) Danov, K. D.; Basheva, E. S.; Kralchevsky, P. A.; Ananthapadmanabhan, K. P.; Lips, A. The Metastable States of Foam Films Containing Electrically Charged Micelles or Particles: Experiment and Quantitative Interpretation. *Adv. Colloid Interface Sci.* **2011**, *168*, 50−70.
(23) Wasan, D. T.; Nikolov, A. D.; Lobo, L. A.; Koczo, K.; Edwards, D. A. Foams, Thin Films and Surface Rheological Properties. *Prog. Surf. Sci.* **1992**, *39*, 119−154.
(24) Wasan, D. T.; Nikolov, A. D.; Kralchevsky, P. A.; Ivanov, I. B. Universality in Film Stratification Due to Colloid Crystal Formation. *Colloids Surf.* **1992**, *67*, 139−145.
(25) Sethumadhavan, G. N.; Nikolov, A. D.; Wasan, D. T. Film Stratification in the Presence of Colloidal Particles. *Langmuir* **2001**, *17*, 2059−2062.
(26) Zeng, Y.; Grandner, S.; Oliveira, C. L. P.; Thunemann, A. F.; Paris, O.; Pedersen, J. S.; Klapp, S. H. L.; von Klitzing, R. Effect of Particle Size and Debye Length on Order Parameters of Colloidal Silica Suspensions under Confinement. *Soft Matter* **2011**, *7*, 10899−10909.
(27) Denkov, N. D.; Yoshimura, H.; Nagayama, K.; Kouyama, T. Nanoparticle Arrays in Freely Suspended Vitrified Films. *Phys. Rev. Lett.* **1996**, *76*, 2354.
(28) Zeng, Y.; von Klitzing, R. Structuring of Colloidal Suspensions Confined between a Silica Microsphere and an Air Bubble. *Soft Matter* **2011**, *7*, 5329−5338.
(29) Klapp, S. H. L.; Grandner, S.; Zeng, Y.; von Klitzing, R. Charged Silica Suspensions as Model Materials for Liquids in Confined Geometries. *Soft Matter* **2010**, *6*, 2330−2336.
(30) Klapp, S. H.; Zeng, Y.; Qu, D.; von Klitzing, R. Surviving Structure in Colloidal Suspensions Squeezed from 3d to 2d. *Phys. Rev. Lett.* **2008**, *100*, 118303.
(31) Zeng, Y.; Schön, S.; von Klitzing, R. Silica Nanoparticle Suspensions under Confinement of Thin Liquid Films. *J. Colloid Interface Sci.* **2015**, *449*, 522−529.
(32) Prud'homme, R. K.; Khan, S. A. *Foams: Theory, Measurements, and Applications*; CRC Press, 1995; Vol. *57*.
(33) Weaire, D. L.; Hutzler, S. *The Physics of Foams*; Oxford University Press, 1999.
(34) Cohen-Addad, S.; Hohler, R.; Pitois, O. Flow in Foams and Flowing Foams. *Annu. Rev. Fluid Mech.* **2013**, *45*, 241−267.
(35) Perkowitz, S. *Universal Foam: From Cappuccino to the Cosmos*; Walker & Company, 2000.
(36) Cantat, I.; Cohen-Addad, S.; Elias, F.; Graner, F.; Höhler, R.; Pitois, O. *Foams: Structure and Dynamics*; Oxford University Press, 2013.
(37) Kraynik, A. M.; Hansen, M. G. Foam Rheology: A Model of Viscous Phenomena. *J. Rheol.* **1987**, *31*, 175−205.
(38) Larson, R. G. The Elastic Stress in "Film Fluids. *J. Rheol.* **1997**, *41*, 365−372.
(39) Johonnott, E. S., Lxviii. The Black Spot in Thin Liquid Films. *Philos. Mag.* **1906**, *11*, 746−753.
(40) Zhang, Y.; Sharma, V. Domain Expansion Dynamics in Stratifying Foam Films: Experiments. *Soft Matter* **2015**, *11*, 4408−4417.
(41) Zhang, Y.; Yilixiati, S.; Pearsall, C.; Sharma, V. Nanoscopic Terraces, Mesas, and Ridges in Freely Standing Thin Films Sculpted by Supramolecular Oscillatory Surface Forces. *ACS Nano* **2016**, *10*, 4678−4683.
(42) Zhang, Y.; Sharma, V. Nanoridge Formation and Dynamics of Stratification in Micellar Freestanding Films. *Langmuir* **2017**10.1021/acs.langmuir.7b01871.
(43) Von Klitzing, R.; Espert, A.; Asnacios, A.; Hellweg, T.; Colin, A.; Langevin, D. Forces in Foam Films Containing Polyelectrolyte and Surfactant. *Colloids Surf., A* **1999**, *149*, 131−140.
(44) von Klitzing, R.; Thormann, E.; Nylander, T.; Langevin, D.; Stubenrauch, C. Confinement of Linear Polymers, Surfactants, and Particles between Interfaces. *Adv. Colloid Interface Sci.* **2010**, *155*, 19−31.
(45) Horn, R. G.; Israelachvili, J. N. Direct Measurement of Structural Forces between Two Surfaces in a Nonpolar Liquid. *J. Chem. Phys.* **1981**, *75*, 1400−1411.
(46) Israelachvili, J. N.; Pashley, R. M. Molecular Layering of Water at Surfaces and Origin of Repulsive Hydration Forces. *Nature* **1983**, *306*, 249−250.
(47) Mezger, M.; Schröder, H.; Reichert, H.; Schramm, S.; Okasinski, J. S.; Schöder, S.; Honkimäki, V.; Deutsch, M.; Ocko, B. M.; Ralston, J. Molecular Layering of Fluorinated Ionic Liquids at a Charged Sapphire (0001). *Science* **2008**, *322*, 424−428.
(48) Perkin, S.; Albrecht, T.; Klein, J. Layering and Shear Properties of an Ionic Liquid, 1-Ethyl-3-Methylimidazolium Ethylsulfate, Confined to Nano-Films between Mica Surfaces. *Phys. Chem. Chem. Phys.* **2010**, *12*, 1243−1247.
(49) Smith, A. M.; Perkin, S. Switching the Structural Force in Ionic Liquid-Solvent Mixtures by Varying Composition. *Phys. Rev. Lett.* **2017**, *118*, 096002.
(50) Gebbie, M. A.; Smith, A. M.; Dobbs, H. A.; Warr, G. G.; Banquy, X.; Valtiner, M.; Rutland, M. W.; Israelachvili, J. N.; Perkin, S.; Atkin, R. Long Range Electrostatic Forces in Ionic Liquids. *Chem. Commun.* **2017**, *53*, 1214−1224.
(51) Asakawa, H.; Yoshioka, S.; Nishimura, K. I.; Fukuma, T. Spatial Distribution of Lipid Headgroups and Water Molecules at Membrane/Water Interfaces Visualized by Three-Dimensional Scanning Force Microscopy. *ACS Nano* **2012**, *6*, 9013−9020.
(52) Anand, U.; Lu, J.; Loh, D.; Aabdin, Z.; Mirsaidov, U. Hydration Layer-Mediated Pairwise Interaction of Nanoparticles. *Nano Lett.* **2016**, *16*, 786−790.
(53) Boles, M. A.; Engel, M.; Talapin, D. V. Self-Assembly of Colloidal Nanocrystals: From Intricate Structures to Functional Materials. *Chem. Rev.* **2016**, *116*, 11220−11289.
(54) Heslot, F.; Fraysse, N.; Cazabat, A. M. Molecular Layering in the Spreading of Wetting Liquid Drops. *Nature* **1989**, *338*, 640−642.
(55) Wu, P.; Nikolov, A.; Wasan, D. Capillary Dynamics Driven by Molecular Self-Layering. *Adv. Colloid Interface Sci.* **2017**, *243*, 114−120.
(56) Yin, H.; Sibley, D. N.; Thiele, U.; Archer, A. J. Films, Layers, and Droplets: The Effect of near-Wall Fluid Structure on Spreading Dynamics. *Phys. Rev. E: Stat. Phys., Plasmas, Fluids, Relat. Interdiscip. Top.* **2017**, *95*, 023104.

DOI: 10.1021/acsnano.7b05391
ACS Nano 2018, 12, 1050−1061

(57) Popescu, M. N.; Oshanin, G.; Dietrich, S.; Cazabat, A. M. Precursor Films in Wetting Phenomena. *J. Phys.: Condens. Matter* **2012**, *24*, 243102.
(58) Richetti, P.; Kekicheff, P. Direct Measurement of Depletion and Structural Forces in a Micellar System. *Phys. Rev. Lett.* **1992**, *68*, 1951.
(59) Sharma, A.; Walz, J. Y. Direct Measurement of the Depletion Interaction in a Charged Colloidal Dispersion. *J. Chem. Soc., Faraday Trans.* **1996**, *92*, 4997−5004.
(60) Trokhymchuk, A.; Henderson, D. Depletion Forces in Bulk and in Confined Domains: From Asakura−Oosawa to Recent Statistical Physics Advances. *Curr. Opin. Colloid Interface Sci.* **2015**, *20*, 32−38.
(61) Asakura, S.; Oosawa, F. On Interaction between Two Bodies Immersed in a Solution of Macromolecules. *J. Chem. Phys.* **1954**, *22*, 1255−1256.
(62) Edwards, T. D.; Bevan, M. A. Depletion-Mediated Potentials and Phase Behavior for Micelles, Macromolecules, Nanoparticles, and Hydrogel Particles. *Langmuir* **2012**, *28*, 13816−13823.
(63) Sonin, A. A.; Langevin, D. Stratification Dynamics of Thin Films Made from Aqueous Micellar Solutions. *Europhys. Lett.* **1993**, *22*, 271.
(64) Tabor, R. F.; Lockie, H.; Chan, D. Y.; Grieser, F.; Grillo, I.; Mutch, K. J.; Dagastine, R. R. Structural Forces in Soft Matter Systems: Unique Flocculation Pathways between Deformable Droplets. *Soft Matter* **2011**, *7*, 11334−11344.
(65) Tulpar, A.; Van Tassel, P. R.; Walz, J. Y. Structuring of Macroions Confined between Like-Charged Surfaces. *Langmuir* **2006**, *22*, 2876−2883.
(66) Kolaric, B.; Jaeger, W.; Hedicke, G.; von Klitzing, R. Tuning of Foam Film Thickness by Different (Poly)Electrolyte/Surfactant Combinations. *J. Phys. Chem. B* **2003**, *107*, 8152−8157.
(67) Beltrán, C. M.; Guillot, S.; Langevin, D. Stratification Phenomena in Thin Liquid Films Containing Polyelectrolytes and Stabilized by Ionic Surfactants. *Macromolecules* **2003**, *36*, 8506−8512.
(68) Beltran, C. M.; Langevin, D. Stratification Kinetics of Polyelectrolyte Solutions Confined in Thin Films. *Phys. Rev. Lett.* **2005**, *94*, 217803.
(69) Beltramo, P. J.; Van Hooghten, R.; Vermant, J. Millimeter-Area, Free Standing, Phospholipid Bilayers. *Soft Matter* **2016**, *12*, 432410.1039/C6SM00250A.
(70) Lalchev, Z.; Todorov, R.; Exerowa, D. Thin Liquid Films as a Model to Study Surfactant Layers on the Alveolar Surface. *Curr. Opin. Colloid Interface Sci.* **2008**, *13*, 183−193.
(71) Oswald, P.; Pieranski, P. *Smectic and Columnar Liquid Crystals: Concepts and Physical Properties Illustrated by Experiments*; CRC Press, 2005.
(72) Pieranski, P.; Beliard, L.; Tournellec, J.-P.; Leoncini, X.; Furtlehner, C.; Dumoulin, H.; Riou, E.; Jouvin, B.; Fénerol, J.-P.; Palaric, P. Physics of Smectic Membranes. *Phys. A* **1993**, *194*, 364−389.
(73) Kralchevsky, P. A.; Nikolov, A. D.; Wasan, D. T.; Ivanov, I. B. Formation and Expansion of Dark Spots in Stratifying Foam Films. *Langmuir* **1990**, *6*, 1180−1189.
(74) Anachkov, S. E.; Danov, K. D.; Basheva, E. S.; Kralchevsky, P. A.; Ananthapadmanabhan, K. P. Determination of the Aggregation Number and Charge of Ionic Surfactant Micelles from the Stepwise Thinning of Foam Films. *Adv. Colloid Interface Sci.* **2012**, *183*, 55−67.
(75) Cascão Pereira, L. G.; Johansson, C.; Blanch, H. W.; Radke, C. J. A Bike-Wheel Microcell for Measurement of Thin-Film Forces. *Colloids Surf., A* **2001**, *186*, 103−111.
(76) Patist, A.; Kanicky, J. R.; Shukla, P. K.; Shah, D. O. Importance of Micellar Kinetics in Relation to Technological Processes. *J. Colloid Interface Sci.* **2002**, *245*, 1−15.
(77) Klapp, S. H. L.; Grandner, S.; Zeng, Y.; von Klitzing, R. Asymptotic Structure of Charged Colloids between Two and Three Dimensions: The Influence of Salt. *J. Phys.: Condens. Matter* **2008**, *20*, 20.
(78) Bales, B. L.; Almgren, M. Fluorescence Quenching of Pyrene by Copper (Ii) in Sodium Dodecyl Sulfate Micelles. Effect of Micelle Size as Controlled by Surfactant Concentration. *J. Phys. Chem.* **1995**, *99*, 15153−15162.
(79) Krichevsky, O.; Stavans, J. Confined Fluid between Two Walls: The Case of Micelles inside a Soap Film. *Phys. Rev. E: Stat. Phys., Plasmas, Fluids, Relat. Interdiscip. Top.* **1997**, *55*, 7260.
(80) Krichevsky, O.; Stavans, J. Micellar Stratification in Soap Films: A Light Scattering Study. *Phys. Rev. Lett.* **1995**, *74*, 2752.
(81) Stubenrauch, C. What Do a Foam Film and a Real Gas Have in Common? *ChemPhysChem* **2005**, *6*, 35−42.
(82) Stubenrauch, C.; Strey, R. Phase Diagrams of Nonionic Foam Films: New Interpretation of Disjoining Pressure Vs Thickness Curves. *Langmuir* **2004**, *20*, 5185−5188.
(83) Bélorgey, O.; Benattar, J. J. Structural Properties of Soap Black Films Investigated by X-Ray Reflectivity. *Phys. Rev. Lett.* **1991**, *66*, 313.
(84) Benattar, J. J.; Schalchli, A.; Bélorgey, O. X-Ray Reflectivity Investigation of Newton and Common Black Films. *J. Phys. I* **1992**, *2*, 955−968.
(85) Carnahan, N. F.; Starling, K. E. Equation of State for Nonattracting Rigid Spheres. *J. Chem. Phys.* **1969**, *51*, 635−636.
(86) Kralchevsky, P. A.; Denkov, N. D. Analytical Expression for the Oscillatory Structural Surface Force. *Chem. Phys. Lett.* **1995**, *240*, 385−392.
(87) Henderson, D. An Explicit Expression for the Solvent Contribution to the Force between Colloidal Particles Using a Hard Sphere Model. *J. Colloid Interface Sci.* **1988**, *121*, 486−490.
(88) Monovoukas, Y.; Gast, A. P. The Experimental Phase Diagram of Charged Colloidal Suspensions. *J. Colloid Interface Sci.* **1989**, *128*, 533−548.
(89) Russel, W. B.; Saville, D. A.; Schowalter, W. R. *Colloidal Dispersions*; Cambridge University Press: Cambridge, 1989.
(90) Pieranski, P. Colloidal Crystals. *Contemp. Phys.* **1983**, *24*, 25−73.
(91) Beresford-Smith, B.; Chan, D. Y. C.; Mitchell, D. J. The Electrostatic Interaction in Colloidal Systems with Low Added Electrolyte. *J. Colloid Interface Sci.* **1985**, *105*, 216−234.
(92) Beltramo, P. J.; Vermant, J. Simple Optical Imaging of Nanoscale Features in Free-Standing Films. *ACS Omega* **2016**, *1*, 363−370.

DOI: 10.1021/acsnano.7b05391
ACS Nano 2018, 12, 1050−1061